

# The High Energy Particle Detector (HEPD) for the CSES mission

---

## Roberta Sparvoli for the CSES/HEPD collaboration

University of Rome Tor Vergata and INFN, Italy

E-mail: [roberta.sparvoli@roma2.infn.it](mailto:roberta.sparvoli@roma2.infn.it)

The CSES space mission, lead by a Chinese-Italian collaboration, will study phenomena of electromagnetic nature and their correlation with the geophysical activity, in order to contribute to the monitoring of earthquakes from space. CSES will monitor various physical parameters including electric and magnetic field, ionospheric plasma in-situ and profile disturbances, and high energy particle fluctuations.

CSES satellite will be launched in late 2016 and inserted into a circular Sun-synchronous orbit with 98 degrees inclination and 500 km altitude. Expected lifetime is 5 years. CSES hosts several instruments onboard: 2 magnetometers, an electrical field detector, a plasma analyzer, a Langmuir probe and a particle detector (the High Energy Particle Detector HEPD).

The HEPD, built by the Italian collaboration, will study the temporal stability of the inner Van Allen radiation belts, investigating precipitation of trapped particles induced by magnetospheric, ionospheric and tropospheric EM emissions, as well as by seismo-electromagnetic disturbances. It consists of two layers of triggering plastic scintillators and of a calorimeter constituted by a tower of plastic scintillator counters and a LYSO plane. The direction of the incident particle is provided by two planes of double-side silicon microstrip detectors placed in front of the trigger.

The HEPD is capable of separating electrons and protons and identify nuclei up to Iron; the high-inclination orbit of the satellite allows the telescope to detect particles of different nature during its revolution: galactic cosmic rays, solar energetic particles, particles trapped in the magnetosphere and anomalous cosmic rays. The HEPD scientific scope - besides monitoring the precipitation of trapped particles in the magnetosphere - is therefore studying the low energy component of cosmic rays too.

In this paper a technical description of the HEPD and its main characteristics will be presented.

*The 34th International Cosmic Ray Conference,  
30 July- 6 August, 2015  
The Hague, The Netherlands*

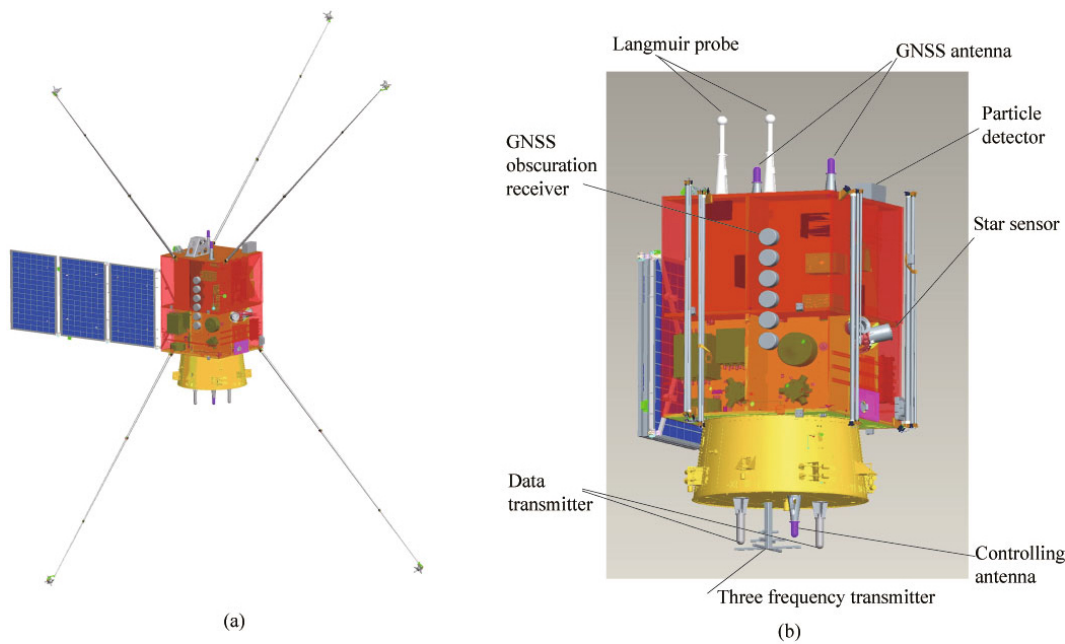


**Figure 1:** Sketch of the CSES satellite. (a) The satellite platform; (b) The position of scientific payloads.

## 1. The CSES mission

Chinese seismologists have been paying great attention to the development of space observation techniques in earthquake science. According to the development of space information technology, the applications of remote sensing in disastrous earthquake, and the requirements of space-ground observation technology for earthquake prevention and disaster mitigation, a comprehensive space-based observation system was proposed to obtain various information from Earth.

The first space-based platform of earthquake stereoscopic monitoring system is the China Seismo-Electromagnetic Satellite CSES [1], which aims to establish a spacebased observation system for detecting electromagnetic anomalies from Earth and ionosphere perturbations possibly associated with earthquakes, to improve the knowledge on earthquakes prediction.

Among the possible anomalies generated by a seismic event, bursts of Van Allen belt electron fluxes in the magnetosphere have been repeatedly reported in literature by various experiments, though a statistical significance was always difficult to claim [2, 3, 4]. A recent study [5] presented a new search for correlation between the precipitation of low energy electrons ( $E > 0.3$  MeV) trapped within the Van Allen Belts and earthquakes with magnitude above 5 Richter scale. The authors used 13 years of electron data measured by the NOAA POES 15, 16, 17 and 18 satellites corresponding to about 18 thousands  $M > 5$  earthquakes registered in the NEIC catalog of the U.S. Geological Survey, and found a correlation peak with significance of 5.7 standard deviations.

In order to establish a firm correlation between the lithosphere and the magnetosphere, the CSES satellite aims at measuring such particle bursts, by means of a particle detector sensitive to sudden bursts and capable of separating electrons from protons.

While flying along the orbit and looking for electron bursts, however, a particle detector aboard

| Item                  | Value                                 |
|-----------------------|---------------------------------------|
| Free field of view    | $\geq 70^\circ$                       |
| Pointing              | Zenith                                |
| Operative temperature | $-10^\circ \pm 45^\circ$              |
| Mass budget           | $< 35 \text{ Kg}$                     |
| Power budget          | $\leq 38 \text{ W}$                   |
| Overall dimensions    | $20 \times 20 \times 40 \text{ cm}^3$ |
| Scientific data bus   | RS-422                                |
| Data handling bus     | CAN 2.0                               |
| Reliability           | 0.99                                  |
| Operating modes       | Survey and Burst                      |
| Lifetime              | $\geq 5 \text{ years}$                |

**Table 1:** HEPD main technical characteristics.

CSES is sensitive to all radiation, not only that coming inside the Earth's magnetosphere. The high-inclination orbit of the satellite allows the telescope to detect particles of different nature during its revolution: galactic cosmic rays - which are modulated by the solar activity at low energies - and also solar energetic particles associated to transient phenomena such as Solar Flares or Coronal Mass Ejections.

The Italian CSES collaboration has a long experience in cosmic ray physics. Its experimental activity, done together with European, Russian and American institutes, started in 1989 with the stratospheric balloon experiments MASS89, MASS91, TS93 and CAPRICE [6, 7, 8, 9, 10, 11] which flew over the years 1989–1994 and whose scientific goal was to measure cosmic rays - with special focus on antimatter - between some hundreds of MeV and few GeVs. The balloon activity was followed by the two satellite experiments NINA and NINA-2 [12, 13] which took data from 1998 until 2003 and were aimed at measuring cosmic ray fluxes of hundreds of MeV.

The major mission of the Italian CSES collaboration is PAMELA [14, 15], a space observatory in orbit since 2006 and still taking data. The main scientific goal of PAMELA is the measurement of cosmic rays (especially antimatter) in the broad energy range from 100 MeV until a few TeV.

Flying on the CSES satellite gives the Italian collaborators the opportunity to repeat the measurements of the two NINA missions (similar orbit, same energy window), in a different period of the solar cycle. This will allow a detailed analysis of solar modulation. CSES will also complement the cosmic ray measurements of PAMELA at low energy, thus giving a complete picture of the cosmic ray radiation by direct measurements from the very low energies (few MeVs) up to the the TeV region.

The strong interest of the Chinese space agency for the development of technologies for monitoring disasters, especially for their own territory, and the interest of Italian researchers to collect data of cosmic rays at low energies due to their long tradition in cosmic ray physics, met together to establish a new collaboration between Italy and China for the construction of a major new satellite

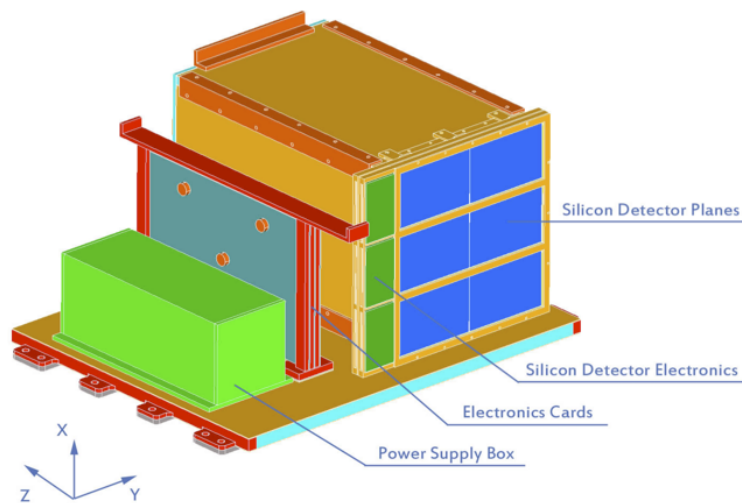


**Figure 2:** View of the HEPD electric box and detector

(the China Seismo-Electromagnetic Satellite - CSES) dedicated to the study of the electromagnetic environment of the Earth.

A memorandum of understanding between the Chinese National Space Administration (CNSA) and the Agenzia Spaziale Italiana (ASI), concerning cooperation on CSES, has been signed on September 25, 2013. The Italian contribution to the CSES mission consists of an innovative instrument (the High Energy Particle Detector HEPD) for measuring energetic particles that precipitate from the Van Allen belts as a result of electromagnetic interference. In addition to this physics goal, the HEPD is an instrument for cosmic rays physics at low energy, taking data along a polar orbit and so able to collect cosmic, solar and trapped particles in space.

The satellite is based on the Chinese CAST2000 platform (see figure 1). It is a 3-axis attitude stabilized satellite and will be placed in a 98 degrees inclination Sun-synchronous circular orbit, at an altitude of 500 km, for a launch scheduled at the end of 2016. Expected lifetime is 5 years.

CSES hosts several instruments onboard: 2 magnetometers, the electrical field detector (EFD), a plasma analyzer, a Langmuir probe and the High Energy Particle Detector (HEPD).

## 2. Description of the HEPD detector

HEPD detector will measure electrons, protons and light nuclei along CSES orbit. The main characteristics of the instrument are reported in Table 1: the detector has a mass of 35 kg, a power consumption of less than 38 W and mechanical dimensions roughly  $20 \times 20 \times 40 \text{ cm}^3$ .

The HEPD detector consists of two layers of plastic scintillators for trigger (one thin segmented counter S1 and one deep counter S2) and a calorimeter. The direction of the incident particle is provided by two planes of double-side silicon microstrip detectors. The silicon tracker planes are placed at the top of detector to limit the effect of Coulomb multiple scattering on the direction measurement. The calorimeter consists of a tower of scintillator counters, 16 layers of plastic scintillator planes ( $15 \times 15 \times 1 \text{ cm}^3$ ) read out by photomultiplier tubes (PMTs), followed by

a  $3 \times 3$  matrix of an inorganic scintillator LYSO (for a resulting plane of dimension  $15 \times 15 \times 4$  cm<sup>3</sup>) read out by PMTs. The calorimeter volume is surrounded by 5 mm thick plastic scintillator veto planes. The main Power Supply must provide the low voltages to the detector electronics and the high bias voltages for PMTs and silicon modules. The basic detector design is shown in Fig. 2.

The HEPD detector is contained in an aluminium box. The walls and the base plate are made of aluminium honeycomb plates. The outside surface is covered with aluminized polyimide layer to assure a good thermal insulation. The detector itself and the power supply system box are both fixed on the base plate.

The Italian groups are developing the Electrical, Mechanical&Thermal, Qualification and Flight Models of the High Energy Particle Detector.

### 3. Simulations

In order to estimate the HEPD performance, a Monte Carlo simulation was developed, based on the Geant4 toolkit to reproduce the detector and the interaction of particles inside. The geometry used for the simulation consists of all active detectors (silicon tracker, trigger planes, calorimeter and veto scintillators) with the material of the mechanical supports plus the top HEPD box and the front satellite wall (fig. 3, left panel).

Protons and electrons were generated from a rectangular surface placed above the satellite wall and large enough to assure particle incoming angles in the range  $0^\circ \leq \theta < 90^\circ$ , where  $\theta$  is the angle between the particle direction and Z-axis. Five million particles were simulated at fixed energy bins (from 30 to 500 MeV for protons and from 1 to 200 MeV for electrons) and hundred million particles were generated according to a power law spectrum. Different trigger configurations were used in order to study the variation on the acceptance windows and consequently on the event rate.

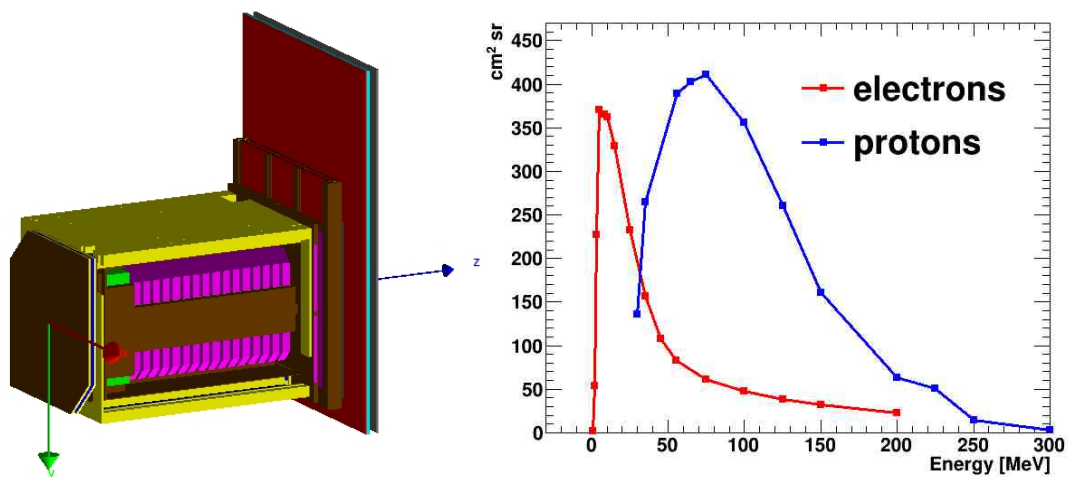


**Figure 3:** LEFT: HEPD simulated geometry. One veto plane has been removed to show the calorimeter inside. The red and grey planes at the top of the apparatus (higher value of Z) are respectively the box in which the HEPD is contained and the satellite wall. RIGHT: Energy acceptance for protons and electrons

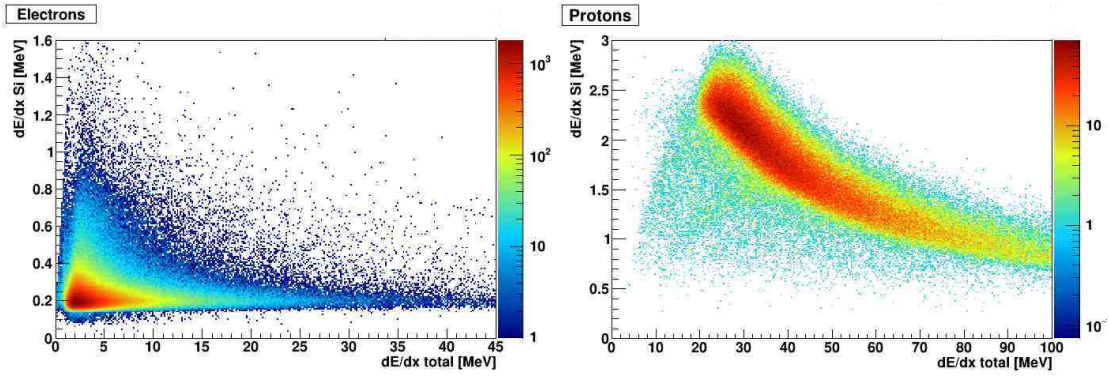


**Figure 4:** Distributions of the energy loss in the silicon tracker and the total energy loss in the detector for electrons and protons.

The angle-integrated electron and proton acceptances are presented in fig. 3, right panel. As a results of the simulations, the energy acceptance window for electrons is between 3 and 200 MeV and for protons between 30 and 300 MeV.

The HEPD provides a good separation between protons and electrons. In the energy range of the detector, protons are slow and not relativistic. For this reason, we used the  $\Delta E$  vs  $E$  method for the  $e^-/p^+$  discrimination, where  $\Delta E$  is the energy deposited in a small thickness of the detector and  $E$  the energy released in the whole detector. The two layers of silicon tracker were chosen as small thickness and the sum of the energy released in the two planes was used as  $\Delta E$ . The resulting 2-dimensional plots for electrons and protons are shown in fig. 4, left and right respectively. We can see that the distributions are very different and particles lay in separate energy bands.

In order to estimate the proton contamination in the electron sample, different selection cuts have been implemented with efficiencies at 90%, 95% and 99% in the electron selection. The three curves used to select electrons are shown in fig. 5. The values of the ratio between 95% confidence level upper limit of background protons [16] surviving the cuts and the number of selected electrons are reported in tab. 2 for different energies.

Table 3 summarizes the main physical characterists of the HEPD, obtained by Montecarlo simulations.

| $E$ [MeV] | p/e (90% cut)         | p/e (95% cut)         | p/e (99% cut)         |
|-----------|-----------------------|-----------------------|-----------------------|
| 2-3       | $< 2.5 \cdot 10^{-5}$ | $< 2.3 \cdot 10^{-5}$ | $< 2.3 \cdot 10^{-5}$ |
| 5-6       | $< 9 \cdot 10^{-5}$   | $< 8 \cdot 10^{-5}$   | $< 1 \cdot 10^{-4}$   |
| 6-10      | $< 5 \cdot 10^{-5}$   | $< 5 \cdot 10^{-5}$   | $< 1 \cdot 10^{-4}$   |
| 10-15     | $< 1.5 \cdot 10^{-4}$ | $< 1.7 \cdot 10^{-4}$ | $< 4 \cdot 10^{-4}$   |
| 15-40     | $< 2.7 \cdot 10^{-4}$ | $< 3.4 \cdot 10^{-4}$ | $< 7 \cdot 10^{-3}$   |

**Table 2:** Protons contaminating the electron signal for three different selection cuts. The values have been obtained considering the upper limits in the proton counts at 95% confidence level [16].

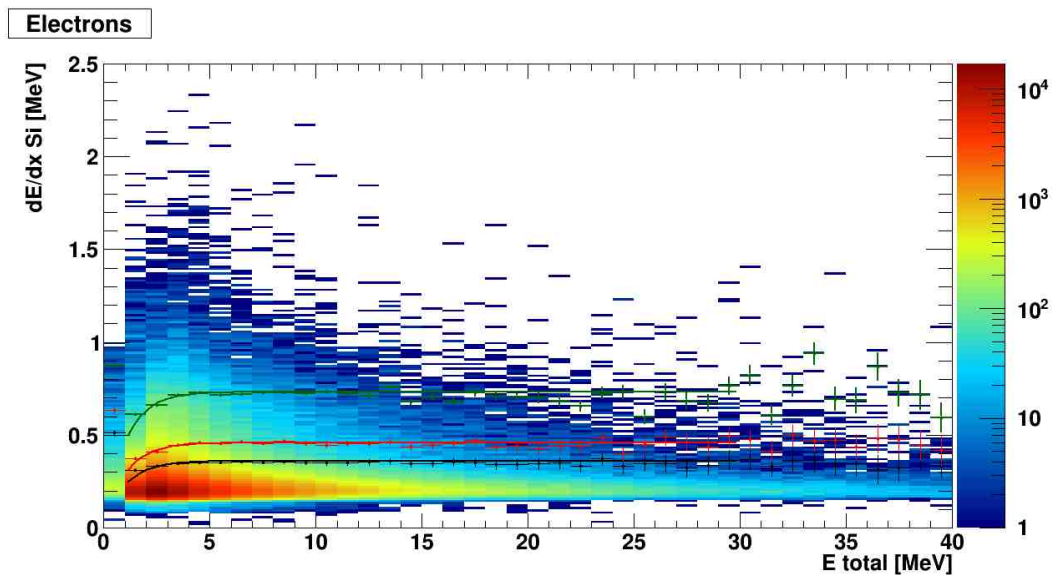


**Figure 5:** Selection cuts in the electron sample with efficiencies at 90% (black) , 95% (red) and 99% (green).

Figure 6 presents the expected count rates for electrons and protons along CSES orbit. Such count rates have been determined taking as incoming fluxes those measured by the MEPED telescope of the NOAA 15 satellite, extrapolated with a power law of index  $\gamma = -2.2$  for electrons and of index  $\gamma = -2.7$  for protons.

#### 4. Schedule and milestones

According to Chinese space procedures, HEPD must be produced in 4 different version: an Electrical Model (EM), a Structural and Mass Model (SMT), a Qualification Model (QM) and a Flight Model (FM).

The EM was sent from Italy to China in July 2014 for electrical tests. The STM was instead shipped in February 2015 and is now undergoing vibration and thermal tests in the Chinese facilities.

The delivery of the QM is scheduled for November 2015 and the final FM will be sent to China by February 2016. The CSES launch is foreseen by Fall 2016.

| Item                          | Value                                 |
|-------------------------------|---------------------------------------|
| Energy range (electrons)      | $3 \text{ MeV} \pm 200 \text{ MeV}$   |
| Energy range (protons)        | $30 \text{ MeV} \pm 300 \text{ MeV}$  |
| Angular resolution            | $8^\circ$ at $E \geq 5 \text{ MeV}$   |
| Energy resolution (electrons) | $\leq 10\%$ at $E \sim 5 \text{ MeV}$ |

**Table 3:** Table with HEPD main physical parameters.

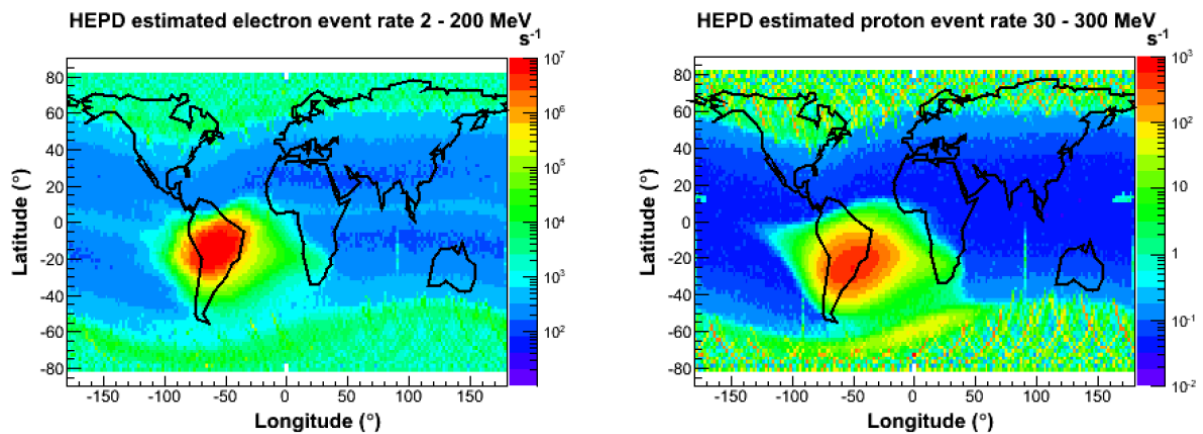


**Figure 6:** Expected rates for electrons and protons along the orbit.

## References

- [1] X. Shen et al, Earthq Sci (2011) 24: 639–650.
- [2] X. Zhang et al, Nat. Hazards Earth Syst. Sci., 13, 197–209, 2013.
- [3] V. Sgrigna, et al 2005, Journal of Atmospheric and Solar- Terrestrial Physics, 67 1448S.
- [4] S. Y. Alexandrin et al 2003, Annales Geophysicae 21, 597.
- [5] R. Battiston, V. Vitale, Nuclear Physics B Proceedings Supplement 00 (2013) 1–10.
- [6] R.L. Golden, et al., Astrophys. J. 436 (1994) 769.
- [7] M. Hof, et al., Astrophys. J. 467 (1996) L33.
- [8] R.L. Golden, et al., Astrophys. J. 457 (1996) L103.
- [9] M. Boezio, et al., Astrophys. J. 487 (1997) 415.
- [10] J. Kremer, et al., Phys. Rev. Lett. 83 (1999) 4241.
- [11] M.L. Ambriola, et al., Nucl. Phys. B - Proc. Suppl. 78 (1999) 32.
- [12] V. Bidoli, et al., Astrophys. J. Suppl. 132 (2001) 365.
- [13] G. Furano, et al., Adv. Space Res. 31 (2003) 351.
- [14] P. Picozza et al, Astroparticle Physics 27 (2007) 296–315
- [15] O. Adriani et al, Physics Reports, 544, 4, 323-370 (2014).
- [16] N. Gehrels, Astrophys. J. , 303:336-346, April 1986.